Electronic Materials Letters, Vol. 5, No. 4 (2009), pp. 157-168
DOI: 10.3365/eml.2009.12.157

Buckling-Based Measurements of Mechanical Moduli of Thin Films

Si-Woo Hahm, Hyun-Sik Hwang, Donyoung Kim, and Dahl-Young Khang*

Department of Materials Science and Engineering, Yonsei University,
262 Seongsanno, Seodaemun-gu, Seoul 120-749, Korea

The buckling-based measurement of mechanical properties of material is reviewed here, which is a very useful technique for the characterization of thin films, nano- or molecular-scale materials, etc. This method is shown to be useful to measure elastic moduli of various thin films such as polymers, polyelectrolyte multilayers (PEM), single-wall carbon nanotubes (SWNT) and millimeter-thick polymer network substrates. Further, it is also shown that the mechanical properties of various organic electronic materials, which may find wide applications in flexible and/or stretchable electronic devices, can be measured by the buckling method. Due to its fast, simple nature, the method can be extended to many other materials, especially to materials existing in thin film form only. The method would be a valuable, complementary technique in mechanical characterization of materials to be added to existing methods such as tensile testing, nano-indentation, and other methods.

Keywords: buckling, elastic modulus**,** organic semiconductor materials

1. INTRODUCTION

Thin film, nano- or molecular-scale materials are being widely used in various fields of science and engineering, such as micro-/nano-electromechanical systems (MEMS/ NEMS),[1,2] functional coatings,[3] actuators[4] and sensors,[5,6] membranes,[7] as well as micro- or macro-electronics.[8] Most of the traditional mechanical property measurement methods, such as tensile testing rely on macro-scale manipulation of a sample and this type of preparation of a specimen is very difficult.[9] Because thin films can be shown to have properties different from those of bulk materials,[10,11] and the mechanical properties of materials are a crucial factor in determining the successful implementation of pre-designed performance and reliability,[12] there is a great need for appropriate metrologies for thin films.

There are many methods for determining the mechanical properties of thin films: Wafer curvature methods,[13] substrate bending method,[14] Brillouin light scattering (BLS),[15-17] and especially nanoindentation.[18-21] But these methods required complex processes and/or expensive equipment.

In this review article, a buckling-based method to characterize the mechanical properties of materials is presented. It will be shown that the buckling method is a very simple and fast yet quite accurate technique to use in characterizing the mechanical properties of various materials. In particular, the method is quite suitable for (ultra)thin films and nano- or molecular-scale materials, which may not exist in bulk form or may be very difficult to prepare a bulk sample of, due to its high cost.

*Corresponding author: dykhang@yonsei.ac.kr

2. BUCKLING OF STIFF FILM ON COMPLIANT SUBSTRATE

Buckling can be found everywhere in our daily life, from macro-scale buckling in aging human skin, the dried skins of fruits, to molecular-scale buckling, such as monolayer.[22-24] The mechanism of buckling has been investigated by many research groups.[25-28] Since the pioneering work of Whitesides and co-workers at Harvard University,[29] there has been renewed interest worldwide due to the useful applications of buckling such as in metrology and stretchable electronics.[30]

A stiff, thin-film layer is prepared on a relatively thick, compliant substrate such as elastomer polydimethylsiloxane (PDMS). When compression is applied to the sample, buckling instability is induced. In general, a stiff film exhibits a long wavelength when buckled, because it expends less energy than buckling into a rather short wavelength. On the other hand, the soft substrate tends to have a shorter wavelength due to its lower energy cost.

Therefore, the buckling wavelength of a given stiff film on a compliant substrate system takes an intermediate value that is between these long and short wavelengths. This is a wavelength that minimizes the total energy of the system, and this value is dependent on the thickness of the film, as well as the mechanical properties of both film and substrate. From the

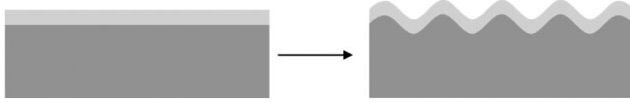

Fig. 1. Schematic drawing for the buckling of a thin film on a compliant substrate.[30]

minimization of the total system energy, which consists of the bending and membrane energies of the film material and the deformation energy of the substrate, it can be shown that the wavelength (λ), amplitude (A) of buckling, and critical strain to induce buckling (ε_{cri}) are given as

$$\lambda = 2\pi h\left(\frac{\overline{E}_f}{3\overline{E}_s}\right)^{\frac{1}{3}},\ A = h\sqrt{\frac{\varepsilon}{\varepsilon_c}-1},\ \varepsilon_{cri} = \frac{1}{4}\left(\frac{3\overline{E}_s}{\overline{E}_f}\right)^{\frac{2}{3}} \quad (1)$$

Here, h is the film thickness, and $\overline{E}$ is the plane-strain modulus ($\overline{E} = E/(1-\nu^2)$). The subscripts f and s mean film and substrate, respectively. ε is the externally applied strain. Using these equations, there are many possible transformations that are useful to evaluate other properties. For example,

$$\overline{E}_f = 3\overline{E}_s\left(\frac{\lambda}{2\pi h}\right)^3,\ \overline{E}_s = \frac{\overline{E}_f}{3}\left(\frac{\lambda}{2\pi h}\right)^{-3},\ h = \frac{\lambda}{2\pi}\left(\frac{3\overline{E}_s}{\overline{E}_f}\right) \quad (2)$$

Equation 2 can be used to evaluate Young's modulus of thin film, Young's modulus of substrate, and the thickness of thin film, respectively.

3. MECHANICAL MODULUS OF THIN FILM

Although the mechanical properties of submicron thin film are crucial for their various applications, many conventional mechanical measuring techniques are not appropriate to measure the forces in straining thin polymer film. Nano-indentation has been used for ceramics and metals, but it is difficult to adopt with soft materials, especially on their submicron thin film forms. Scanning probe microscopy (SPM) can be used to measure the elastic moduli of polymer films, but the accuracy of results using this method is limited due to uncertainty about the tip size and/or contact area. Furthermore, most available methods have low throughput and require specialized instruments and personnel. So, Stafford and colleagues at the National Institute of Standards and Technology (NIST)[31] demonstrated a novel technique based on the mechanical buckling phenomenon, also called strain-induced elastic buckling instability for mechanical measurements (SIEBIMM), because this technique can rapidly and easily measure the elastic moduli of thin films.

A silicon wafer was cleaned with a UV source to make the hydrophilic surface and then spin-cast polystyrene film on it for uniform coating, while flow coating was applied for the preparation of film having thickness gradient. Thin film was transferred to PDMS elastomeric substrate by water immersion method. This PS/PDMS sample was compressed at both ends to induce buckling and buckling wavelengths were checked by small-angle light scattering (SALS), atomic force microscopy (AFM). The mechanical modulus of thin PS film measured by the buckling method was compared to the value obtained from nano-indentation experiments. As shown in Fig. 2, buckling wavelength is sensitive to the thickness change of PS film, and the elastic modulus using Eq. 1 is ~3.5 GPa, which is very consistent with the reported bulk values.

Figure 3 shows the measured moduli values as a function of plasticizer concentration for thin PS films, which confirmed the accuracy of the buckling-based method. The buckling and nano-indentation measurements show the same tendency and are well in accordance within a margin of experimental error. But, above 20% concentration, due to diffusion of plasticizer from thin film to PDMS, a discrep-

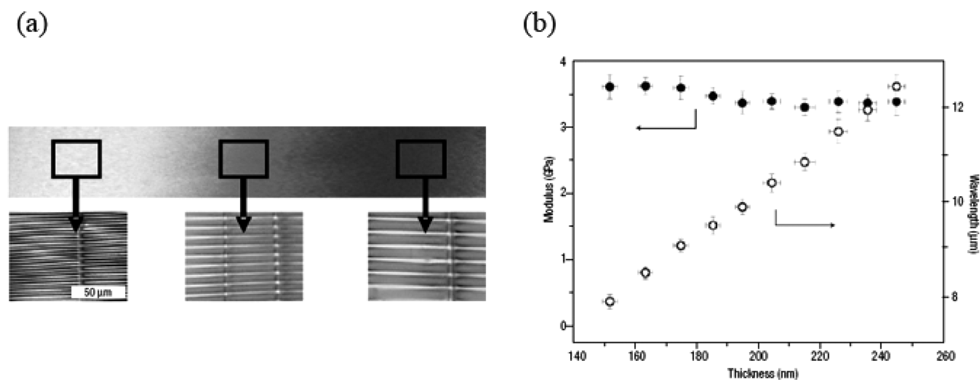

Fig. 2. Modulus measurements of a thickness gradient film of PS.[31] (a) Optical micrograph of a PS thickness gradient on silicon wafer (140 nm to 280 nm). Greyscale insets show optical micrographs of the film after transfer to PDMS and application of strain to induce buckling. The doubling of the film thickness from left to right results in a doubling of the buckling period. (b) Modulus versus thickness for a flow-coated thickness gradient sample. The linear increase in buckling wavelength (open circles) with film thickness confirms that the wrinkling instability is consistent with Eq. 1. The modulus (filled circles) remains largely constant (3.4 ± 0.1 GPa) over this thickness range, in good agreement with the reported bulk values. The error bars represent one standard deviation of the data, which is taken as the experimental uncertainty of the measurement.

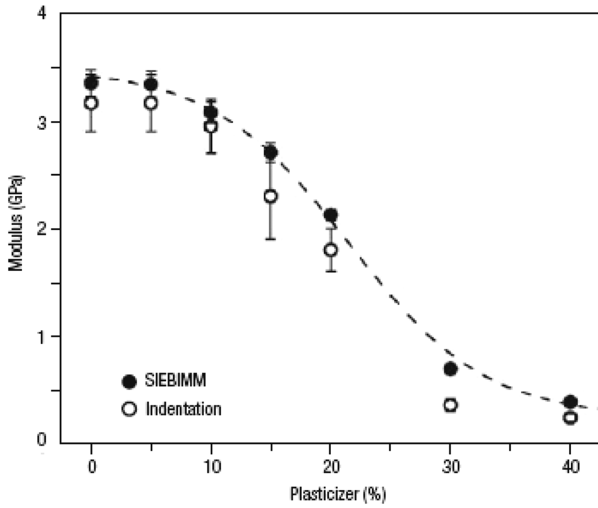

Fig. 3. Modulus versus plasticizer concentration (dioctyl phthalate) for thin PS films.[31] SIEBIMM measurements (filled circles) and nanoindentation measurements (open circles) showing the modulus decreases monotonically with increasing concentration of plasticizer in the film. The thickness (h) of the films ranged from 110 nm to 130 nm. The data are fit to a sigmoidal function (dashed line) as a guide to the eye. The error bars represent one standard deviation of the data, which is taken as the experimental uncertainty of the measurement. Some error bars are smaller than the symbols.

ancy starts to appear.

In order to measure the elastic moduli of ultrathin (<100 nm) films that are focused to promising candidates for various technologies such as barrier layers, actuators, sensors, and organic electronics, Stafford et al. adopted SIEBIMM technique for ultrathin PS and poly (methylmethacrylate) (PMMA), and compared the results with those obtained by the BLS method.[32] BLS can be used to measure the elastic modulus of both supported and free-standing thin polymer film. However, the thinner the free-standing film is, the more difficult it is to measure by BLS due to sample preparation and handling issues.

According to these experiments, in the above 40-nm thickness range, the measured value (~4 GPa) of PS film is in good accordance with the result from BLS of PS film (3.72 GPa) and bulk PS (3.48 GPa), and theoretical value by Eq. 1. But below 40-nm thickness, an unexpected decrease of moduli was apparent. This is a clear breakdown of Eq. 1 for ultrathin film, so they proposed a composite model to include a thin surface layer of thickness δ having a modulus, $\overline{E}_f$, different than the bulk modulus, $\overline{E}_f$. The effective modulus $\overline{E}_f$ is used instead of $\overline{E}_f$ in Eq. 1 for this composite film. This modeling can predict the decrease of modulus below 40 nm thickness range, as shown in Fig. 4(a).

This can be considered to be a pertinent model, considering that the molecular structure and dynamics at the surface of a film can be different from that in the bulk. It can be better understood by taking into account the effect of the surface region. For thick film, wavelength is not sensitive to this small area. But for ultrathin film, the surface region is nearly 40% of the total film thickness and thus sensitive to the surface. The computed decrease of moduli can be confirmed by the result of experiments that contain various molecular weight and material, as in Fig. 4(b).

Nolte *et al.* at the Massachusetts Institute of Technology (MIT) have focused on buckling-based measurement of polyelectrolyte multilayers (PEM).[33] PEM deposition is a technique in which two or more oppositely charged water-soluble polymers are adsorbed onto a substrate in layer-by-layer fashion. PEMs are widely used as matrix materials for enzymes and proteins in sensor applications, matrices for active components in solar cells, permeable membranes for nano-filtration, and fabrication of thin-walled hollow micro-

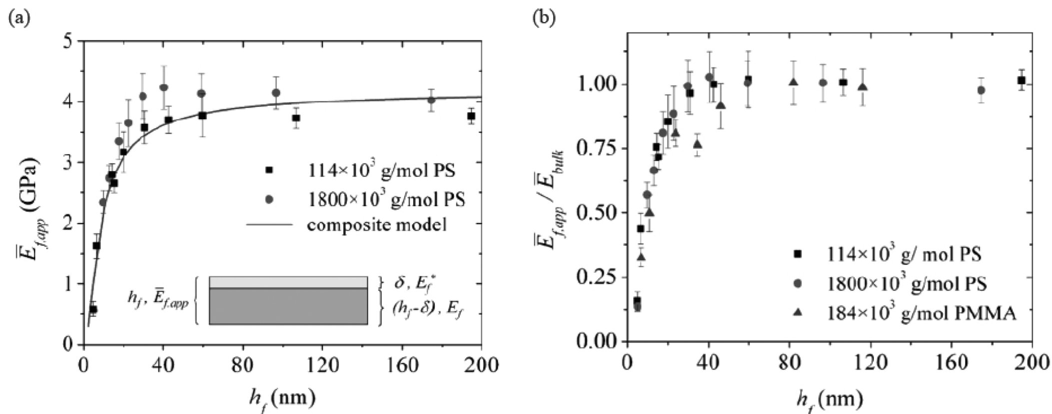

Fig. 4. (a) Apparent modulus ($\overline{E}_{f,app}$) as a function of thickness (h_f) for PS films having M_w=114×103 g/mol (■) and M_w=1800×10^3 g/mol (●). The solid blue line is $\overline{E}_f$ for a composite film having $\overline{E}_f$=4.2 GPa, $\overline{E}_f^*$=0.1 GPa, and δ=2 nm. The error bars represent one standard deviation of the data, which is taken as the experimental uncertainty of the measurement. (b) Reduced modulus ($\overline{E}_{app}/\overline{E}_{bulk}$) for the two PS (■, ●) and PMMA (▲) materials as a function of thickness (h_f). The error bars represent one standard deviation of the data, which is taken as the experimental uncertainty of the measurement.[32]

and nano-capsules that can be used for controlled drug delivery. These wide applications of PEM have become increasingly popular, thus a precise and simple measurement method for their mechanical properties is of great importance.

Conventional metrologies may be applied for a micron-scale film thickness. Considering that certain PEM systems may exhibit thickness increments of less than 1nm/bilayer,[34] conventional methods become impractical. Thus, Nolte's team used the buckling method to measure the modulus of PEM assemblies. The films consisting of poly (allylamine-hydrochloride) (PAH) and poly-(styrenesulfonate) (PSS) on PDMS was chosen for testing. Constructed multilayer films by usual manner were compressively strained with a pair of tweezers during examination of the film using an optical microscope (OM). This OM image was Fourier transformed, and strain induced buckling wavelength was obtained from the transformation. With these wavelengths, film thickness which measured by spectroscopic ellipsometry, and Poisson's ratio (0.33 for dry-state, 0.5 for wet-state), the elastic modulus of PEM could be obtained as ~ 4.4±0.7 GPa by Eq. 1 (Fig. 5(a)).

In addition, PDMS substrate soaked in DI water for six hours before beginning multilayer deposition was used to test the sensitivity of the buckling method for substrate-dependent morphology change in PEM films. As shown in Fig. 5(a), PEM films on the soaked PDMS show lower moduli below 40 layers, contrasted to that of the films on untreated PDMS, because surface reconstruction of water-treated PDMS makes the initial absorbing layer to adopt a chain structure different from the untreated PDMS. However, above a certain thickness of films, the surface effect is diminished.

A PEM/PDMS specimen was immersed in DI water and its solution with 1M of NaCl. The results are shown in Fig. 5(b). Because water is a good solvent for PEM films, the higher chain mobility in expanded film induces the large reduction of elastic modulus and has possibility to break and reform electrostatic cross-links. The salt increases this effect by charge screening and causes reconstruction of the film. As a result, the specimen immersed in NaCl solution regained its modulus only 86% after drying.

Results from these experiments have shown two conclusions. First, SIEBIMM is sensitive enough to check the modification of elastic modulus that depends on surface of substrates. Second, adequate thickness of multilayer is required to avoid measurement influenced by substrate–induced effects in ultrathin film (above 40bilayer in this experiment).

Nolte *et al.* also introduced the 'two-plate buckling technique' as a method of measuring modulus of the PEM.[35] PS was spun onto silicon wafer. PS coated side was placed on PDMS surface and immersed under DI water. After removing silicon wafer, PS film remains on PDMS surface. Consequently, the PS coated PDMS has immersed in PAH and PAA in sequence to assemble PEM. PAH and PAA cycles was repeated to control PEM thickness.

Because of hydrophobic nature of PDMS surface, there are many difficulties in assembling PEM on it. There are well known techniques to modify the wetting properties of PDMS surface.[36,37] However, direct surface treatment on PDMS can cause interference with the mechanical properties of PDMS surface. Hence, Nolte et al. have introduced a PS layer to control wettability easily, thus leading to a "two-plate" buckling system. Unlike in the single-layer buckling technique (Fig. 6(a)), they measured the PEM modulus through a PS/PEM two-plate system (Fig. 6(b)). To make a precise calculation of PEM modulus, they suggested modified equations and proved validity of those equations through experiments. Figures 6(c) and (d) show that PEM grown on two-plate system displays linear growth as in the case of single-layer PEM. In addition, the measured moduli from both systems remained almost constant and there was

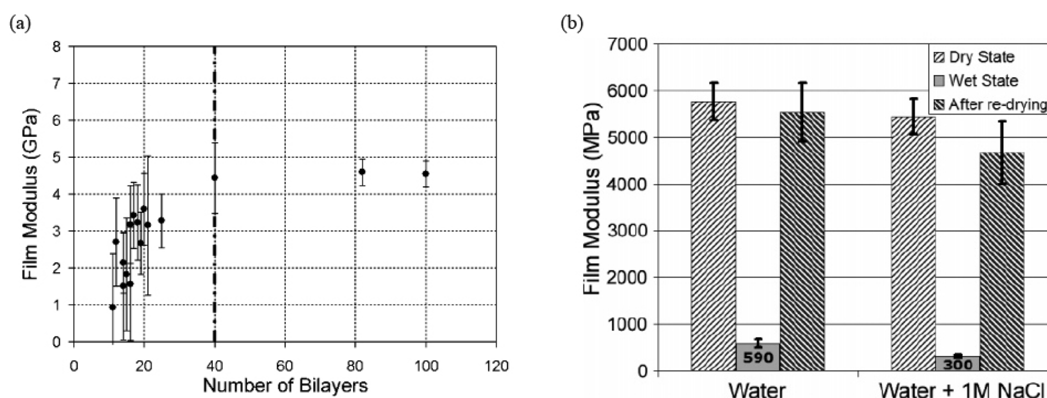

Fig. 5. (a) Effect of substrate treatment on the Young's modulus of PAH/PSS films. PDMS substrates were treated by soaking in DI water for ~6 h prior to multilayer de position. (b) Dry- and wet-state modulus values of PAH/PSS films. Samples with 75 bilayers were tested in both DI water and 1 M NaCl solution. Modulus values of the films following drying of the swollen samples are also shown.[33]

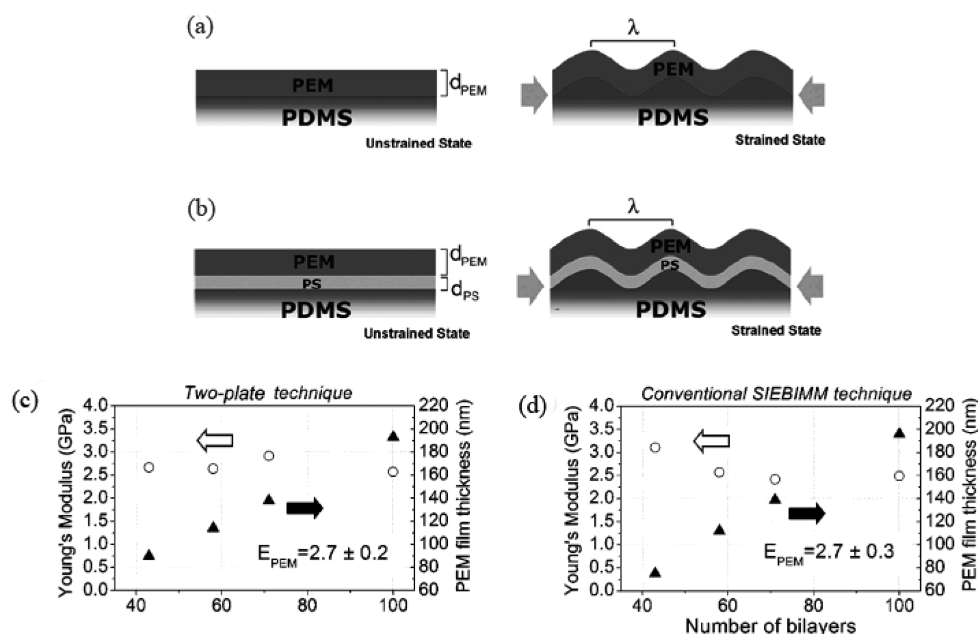

Fig. 6. Cross-sectional illustrations showing both the unstrained and strained (undergoing buckling) states for (a) the conventional SIEBIMM technique with a PEM film and (b) the two-plate method with a PS-PEM composite film. (PAH3.0/PSS3.0) film thickness (filled triangles) and Young's modulus (open circles) vs number of bilayers using the (c) two-plate and (d) conventional SIEBIMM techniques. The average modulus for each technique is displayed in each graph pane. The relative humidity was 50±4%.[35]

perfect correlation of those two values. Furthermore, according to their experiments, humidity conditions play a significant role in the mechanical properties of PEM film. From this perspective, the two-plate buckling technique is a suitable way to measure the PEM modulus because it allows measurements to be performed under a wide range of conditions in terms of humidity.

It is even possible to adopt this buckling-based metrology with polymer brush. Although they have many practical applications, the mechanical properties of polymer brush are challenging, especially on a transparent substrate. Huang *et al*. measured poly (2-hydroxyl methacrylate) (PHEMA) polymer brush layer grafted to the surface of PDMS substrate.[38] In order to introduce hydroxyl groups to the surface of PDMS, which makes a covalent bonding with initiator groups for subsequent polymerization, acid treatment is used instead of conventional oxygen plasma or ultra-violet (UV) ozone treatment due to a lack of noticeable defect even under applied tensile and compressive strains. This process is shown in Fig. 7(a) schematically. The results from this experiment (E=2.6 0.5 GPa, Fig. 7(b)) were in good agreement with literature values (E~2 GPa) for bulk PHEMA at room temperature. Conversely, they also used the buckling wavelength to measure the thickness of polymer brush layer. In comparison with spectroscopic ellipsometry data, the effectiveness of this approach to measure an unknown film's thickness by using known mechanical parameters was also demonstrated.

4. MECHANICAL MODULUS OF SUBSTRATE

It was also shown that the buckling method could be used to measure the mechanical properties of soft polymer network substrate, instead of film properties. Wilder et al. investigated this using PS sensor film of known modulus and thickness.[39]

PS sensor film of which the mechanical properties are known was coated on substrates such as PDMS and cross-linked 2-hydroxyethyl methacrylate (HEMA) hydrogel. Then the Wilder team measured the elastic moduli of these substrates by performing buckling experiments. Using a polymer network that has a discrete gradient in the elastic modulus, they showed how this metrology is suitable to map local differences and heterogeneity in modulus within a sample (Fig. 8).

5. RESIDUAL STRESS IN THIN POLYMER FILMS

Measuring residual stress in thin polymer film is crucial in thin film metrology since the residual stress can be detrimental to thin film coatings and nano-scale devices because of their instability. Although several methods are proposed to measure the residual stress in polymer films, uncertainty about which is best becomes greater as the film thickness decreases. On this matter, Chung *et al*. demonstrated a method of quantifying residual strain in thin polymer films

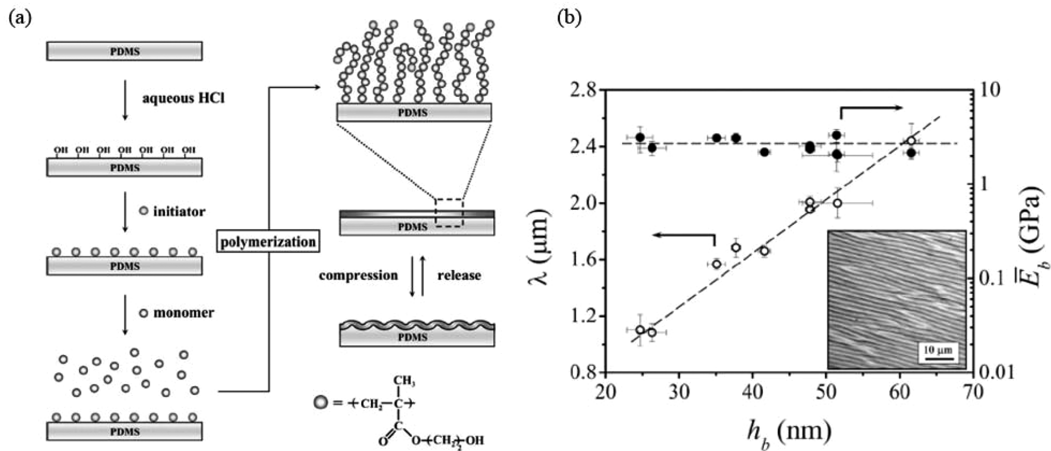

Fig. 7. (a) Illustration of the surface modification of PDMS by surface initiated polymerization, forming a polymer brush layer that extends away from the interface, which can undergo surface wrinkling brought about by either mechanical or thermal compression. (b) Mechanical wrinkling of PDMS-g-PHEMA along a thickness gradient. The wavelength (λ) of the wrinkles, as measured by optical microscopy (see inset), increases linearly with thickness in agreement with Eq. 1, resulting in a constant plane-strain modulus, $\overline{E}_{b,}$) 2.9 (0.6 GPa. Assuming ν_b=0.33, the Young's modulus of the brush layer is E_b=2.6±0.5 GPa. The dashed lines are meant to guide the eye. The error bars represent one standard deviation of the data, which is taken as the experimental uncertainty of the measurement.[38]

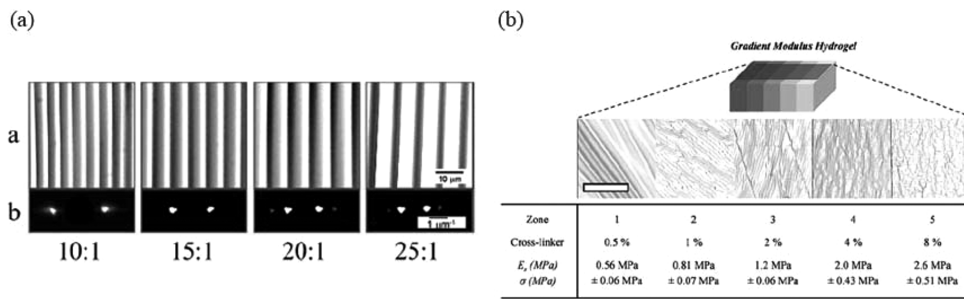

Zone	1	2	3	4	5
Cross-linker	0.5 %	1 %	2 %	4 %	8 %
E_s (MPa) / σ (MPa)	0.56 MPa ± 0.06 MPa	0.81 MPa ± 0.07 MPa	1.2 MPa ± 0.06 MPa	2.0 MPa ± 0.43 MPa	2.6 MPa ± 0.51 MPa

Fig. 8. (a) Buckling patterns for a PS sensor film on PDMS with different mass ratios of base to curing agent as viewed by (A) optical microscopy and (B) small-angle light scattering. (b) (top) Optical microscopy of buckling patterns for a PS sensor film on poly(HEMA) hydrogels comprised of a discrete gradient in the mass fraction of cross-linker in the hydrogel formulation. The scale bar in the optical images is 100 μm. (bottom) The table shows the cross-linker content and corresponding modulus (E_s) and standard deviation (δ) for each zone of the discrete gradient.[39]

by buckling.[40] They used a SALS apparatus to measure buckling wavelength. As laser light is diffracted through the thin polymer layer, it is projected onto a screen and the image acquired by CCD camera. Figure 9(a) shows the intensity of the scattered light from the wrinkled polymer film. Insets there show the strong light intensity of diffracted light patterns when there is wrinkling. This increased intensity implies the onset of buckling, because the point at which the intensity starts to increase indicates the surface is not in a flat, smooth configuration. The buckling wavelength is given by the dominant wave number calculated from the location of the first peaks. Also, the elastic modulus of the film can be estimated by Eq. 1. This modulus was used to determine the theoretical critical strain of buckling (ε_{c0}) in Eq. 1.

The critical buckling strain determined from the theory (i.e., Eq. 1) was three times lower than the experimentally observed critical strain (ε_{cri}). To explain this discrepancy, Chung's team assumed that the critical strain (ε_{cri}) is a sum of the theoretical critical strain (ε_{c0}) and the residual strain (ε_R) as follows:

$$\varepsilon_{cri} = \frac{1}{4}\left(\frac{3\overline{E}_s}{\overline{E}_f}\right)^{\frac{2}{3}} + \varepsilon_R \tag{3}$$

This assumption was confirmed by experimentation, which showed the extinction of residual stress by increasing annealing time and mass fraction of plasticizer.

Therefore, buckling was proved a good method to measure residual stress of thin polymer film. Figures 9(b) and (c) show that the discrepancy in critical strain between theoretical and observed cases can be used to calculate residual stress in thin polymer films. The difference between observed and theoretical stress becomes residual strain of film and this

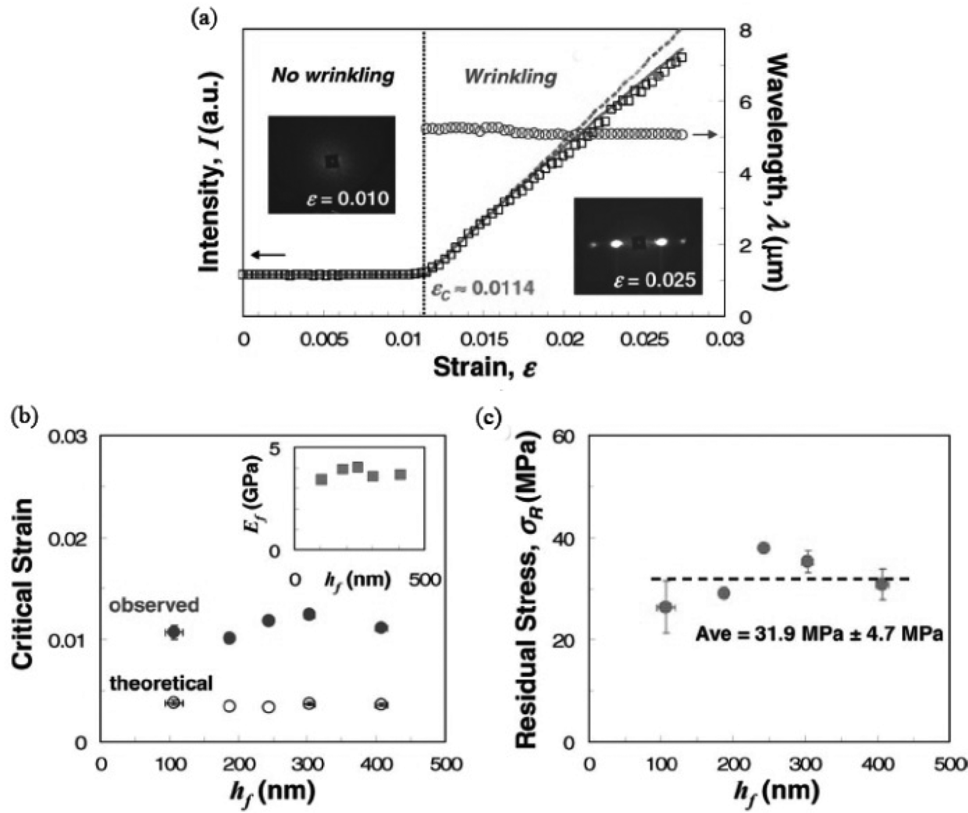

Fig. 9. (a) Representative plot depicting first order diffraction intensity (open squares) versus compressive strain. The insets show the representative SALS diffraction patterns observed below and above the critical strain for the onset of wrinkling (σ_c). The dominant wavenumber (q_0) is measured from the location of the first diffraction peaks, and the wavelength of the wrinkles (λ) is given by $2\pi/q_0$. The wavelength (open circles) is used to determine the Young's modulus of the film by means of Eq. 1. (b) Observed critical strain (closed circles) and theoretical critical strain (open circles) obtained as a function of film thickness (h_f). The inset displays the measured modulus as a function of hf, which was calculated by means of eq 1 with the measured wavelength. (c) Corresponding residual stresses (σ_R) as a function of hf. The dashed line is meant to guide the eye, and the error bars represent one standard deviation of the data, which is taken as the experimental uncertainty of the measurement.[40]

can be converted into residual stress by Eq. 4.

$$\sigma_R = \bar{E}_f \varepsilon_R \tag{4}$$

6. BUCKLING AT MOLECULAR OR NANO SCALE

Khang *et al.* at University of Illinois at Urban-Champaign group have shown the applicability of the buckling method as a nano- or molecular-scale metrology,[41] such as single-wall carbon nano-tubes (SWNT). Their results showed that the manipulation of buckling phenomenon at molecular scale dimensions (~1 nm) is possible. It was notable due to possibility of application to other similar shape of materials such as DNA and RNA.

Arrays of aligned SWNTs having diameters ranging from 1 nm to 4 nm, grown by chemical vapor deposition (CVD) on single-crystal quartz substrate, were transferred to a mechanically pre-strained (3% to 5% tensile strain along the lengths of the SWNT) PDMS substrate. The measured buckling wavelength showed periods of ~160 nm and several nanometers in amplitudes (Fig. 10).

Khang's team also proposed an analytical continuum mechanics theory, and this Newtonian analytical method can elucidate all measurable aspects of this system. They assumed the SWNT as a hollow, elastic tube with outer radius R, thickness t, and elastic modulus E_{CNT}. The out-of-plane displacement of a wavy SWNT shows sinusoidal shape along the length direction, with a height that varies according to $w=A\cos(kx)$, where A is the amplitude and k is the wavevector, with $\lambda=2\pi/k$. The minimization of the total energy of the system with respect to A and k yields the following expressions for the buckling of SWNT

$$k\left(\frac{E_{CNT}I}{\bar{E}_s}\right) = \left[\frac{2\pi(1-\gamma-\ln kR)}{(3-2\gamma-2\ln kR)^2}\right]^{\frac{1}{4}} \tag{5}$$

$$A = \frac{2}{k}\left[\varepsilon_{pre}-\varepsilon_a-\frac{E_{CNT}I}{E_{CNT}S}k^2-\frac{\bar{E}_s\pi}{E_{CNT}Sk^2(3-2\gamma-2\ln kR)}\right]^{\frac{1}{2}} \tag{6}$$

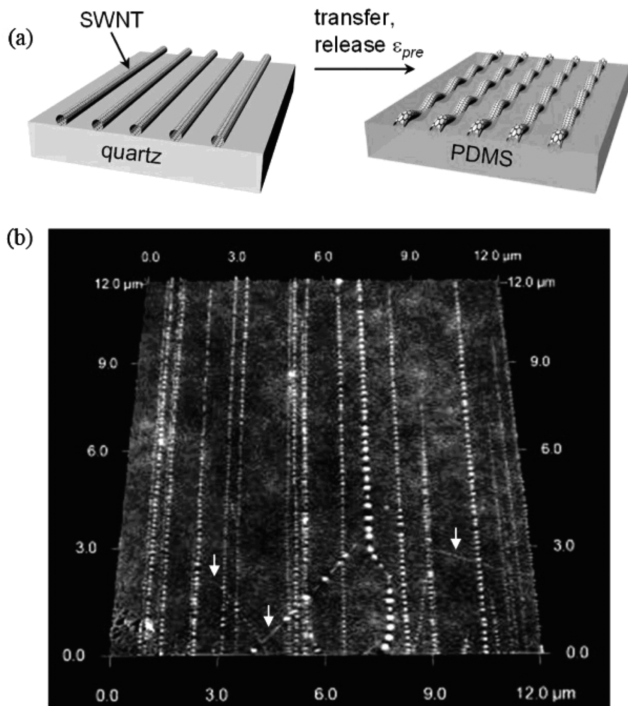

Fig. 10. (a) Transfer of aligned arrays of SWNTs grown on quartz to a uniaxially strained substrate of PDMS followed by release of the pre-strain (ε_{pre}) causes nonlinear buckling instabilities in the SWNT that lead to wavy configurations. (b) Large-area(12 µm×12 µm) angled-view atomic force micro-scope (AFM) image of wavy SWNTs on a PDMS substrate.[41]

where, $\gamma = 0.557$ is Euler's constant, $E_{CNT}I$ and $E_{CNT}S$ are the bending stiffness and tension stiffness of the CNT, respectively. These expressions are valid not only for individual SWNT but also for multi-walled nano-tubes and bundles of SWNTs. According to calculations using these model equations, computed value of the amplitude is 5 nm, and that of elastic modulus is 1.3±0.2 TPa, both of which show good agreement with experimental results (Fig. 11). Success in this model means that Newtonian mechanics is well-suited for precise descriptions of these systems, even when macroscopic concepts such as tube wall thicknesses are molecular scale in dimension.

Carbon-rich networks have recently become an area of major interest due to their possible applications in advanced electronics, nano-mechanics, and other areas. A 2-dimensional carbon nano-material such as graphene is produced by micromechanical exfoliation of bulk graphite (highly ordered pyrolytic graphite, HOPG) or by thermal treatment with silicon carbide.[41-43] Because these conventional methods cannot control the detailed chemistry at the molecular level, Schultz *et al.* proposed a novel method for the synthesis of 2D carbon nano-material.[44] The schematic process for the preparation of 2D carbon-based monolayer film is shown in Fig. 12(a). Firstly, di-functional and hexa-functional aryl alkynes were synthesized. Using this monomer solution, a self-assembled monolayer (SAM) of these materials was formed on SiO_2- or Si_3N_4- coated substrates. Mo-catalyzed, vacuum-driven alkyne metathesis linked the dipropyne SAMs derived from di-functional oligonmer, and Cu-catalyzed Hay-type coupling conditions formed linked monolayer from hexa-functional SAMs. To check the mechanical stability of these cross-linked monolayer films, the buckling method was applied. Transfer of monolayer ribbons to pre-strained PDMS was followed by the release of strain induced nonlinear sinusoidal buckling (Fig. 12(b)). With the known mechanical properties of PDMS and measured thickness of the monolayer, elastic modulus was calculated by Eq. 1, which yielded a result indicating that moduli are between 1 GPa and 10 GPa, which is typical of polymers of similar material.

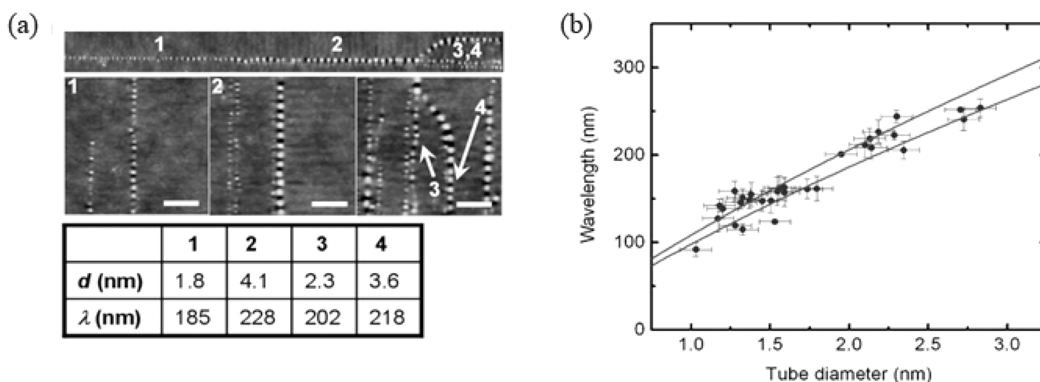

	1	2	3	4
d (nm)	1.8	4.1	2.3	3.6
λ (nm)	185	228	202	218

Fig. 11. (a) AFM images that illustrate the dependence of the wavelength and amplitude on SWNT diameter. Bundles or close clusters of SWNTs lead to spatial variations in the wavelength and amplitude with length. The scale bars are 1 µm; the difference in height between the darkest and lightest regions is 20 nm for all images. (b) Comparison between experimentally measured buckling wavelengths and calculation (lines) in which the Young's modulus of the SWNTs, ECNT, serves as a single variable parameter. The upper and lower curves correspond to a modulus of 1.5 and 1.1 TPa, respectively. On the basis of these results, we conclude that the modulus is 1.3±0.2 TPa.[41]

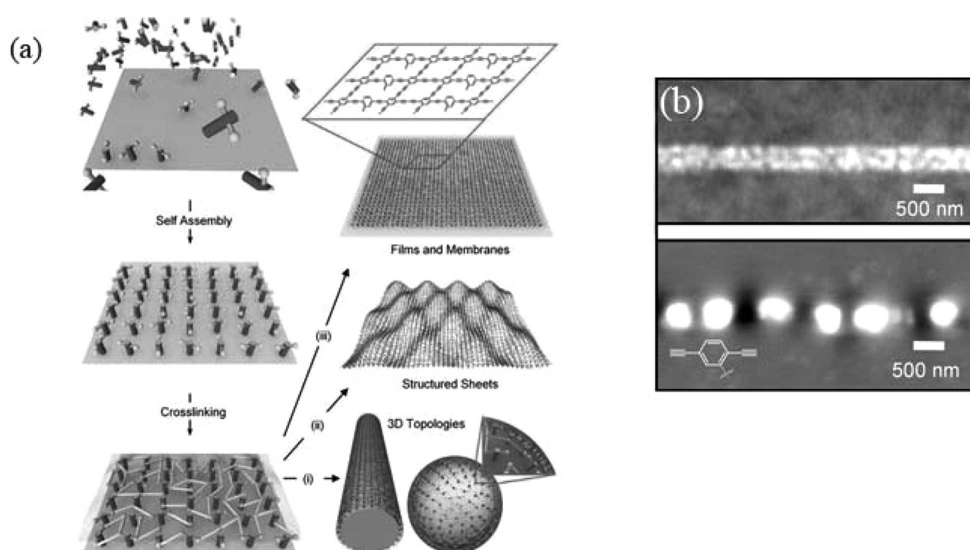

Fig. 12. (a) Self-assembled monolayers (SAMs) are synthesized on a substrate, then cross-linked to form linked monolayers.[44] This approach is applied to the formation of 3D topologies (i), structured sheets (ii), and membranes (iii). The box above iii provides an idealized view of the chemical structure for a linked monomer network. (b) AFM images of a ribbon of a monolayer membrane from 2(width=500 nm) on a pre-strained PDMS substrate before (Upper) and after (Lower) releasing the pre-strain.

7. MECHANICAL MODULUS OF ORGANIC ELECTRONIC MATERIAL

Tahk *et al.* investigated the modulus of organic electronic materials.[45] Due to limitations in fabricating bulk samples of these materials for conventional measurement, SIEBIMM is considered to be a proper method. Poly (3-hexylthiophene) (P3HT) is widely used for transistors and organic light emitting diodes (OLED). Its blend with a fullerene derivative of [6,6]-phenyl C61-butyric acid methyl ether (PCBM) is a material of choice for bulk heterojunction (BHJ) organic solar cell. P3HT and P3HT/PCBM composite material were dissolved in chlorobenzene that swells PDMS significantly, thus it is necessary to make thin film on other substrates and then transfer it onto PDMS. Polymer thin film was coated on a substrate, which has vapor-deposited fluorinated self assembly monolayer (F-SAM) material, tridecafluoro-1,1,2,2-tetrahydrooctyl-trichlorosilane (FOTCS), to ease the following pick-up process. A flat bulk PDMS was laminated on thin polymer film, and detached instantaneously.

In the case of hydrophilic materials such as poly (3,4-Ethylene dioxythiophene): polystyrene-sulfonate (PEDOT:PSS), emeraldine base polyaniline (PANI), which are used for electrodes, electromagnetic shielding device, and charge injection layer, can be directly spun on PDMS substrate which was treated by oxygen plasma to make hydrophilic surface. Pentacene is an active semiconductor in organic thin film transistor due to its high mobility. Pentacene was directly deposited on PDMS by thermal evaporation.

Prepared organic material/PDMS specimens were compressed up to ~2% on a home-made compression stage, under an OM equipped with digital camera. The buckling wavelength was obtained from captured OM images, by averaging 10 to 30 wavelength to decrease the error. AFM was also used to measure buckling wavelength when the wave length was too small to be observed by OM. The obtained value and film thickness that is measured by surface profiler and thickness monitor were substituted in Eq. 1, from which the mechanical properties of organic material was evaluated.

Young's modulus of P3HT was ~1.3 GPa, which is comparable with the literature value of ~0.7 GPa, and that of P3HT/PCBM blend film was significantly increased, ~6.2 GPa (Fig. 13), because PCBM nano-particle plays the role of reinforcing filler.

From the wavelength vs. thickness plot of PEDOT:PSS layer (Fig. 14), elastic modulus was obtained to be ~2.4 GPa. This value is in good agreement with that of literature values (2.5~3.0 GPa). In general, the mixtures of charged polymers such as PEM show 2~3 times lager modulus than their parent homopolymers, due to strong ionic bonding between the layers. The theoretically predicted modulus value of each component (i.e., PEDOT and PSS) is ~3.5 GPa, which is similar to that of PEDOT: PSS. Thus, we can conclude the addition of PEDOT oligomer to PSS matrix on elastic modulus is negligible, mainly due to the very short chain length.

In the case of pentacene, elastic modulus was measured as ~15 GPa. This relatively larger value for pentacene than other polymers is thought to be originated from its polycrys-

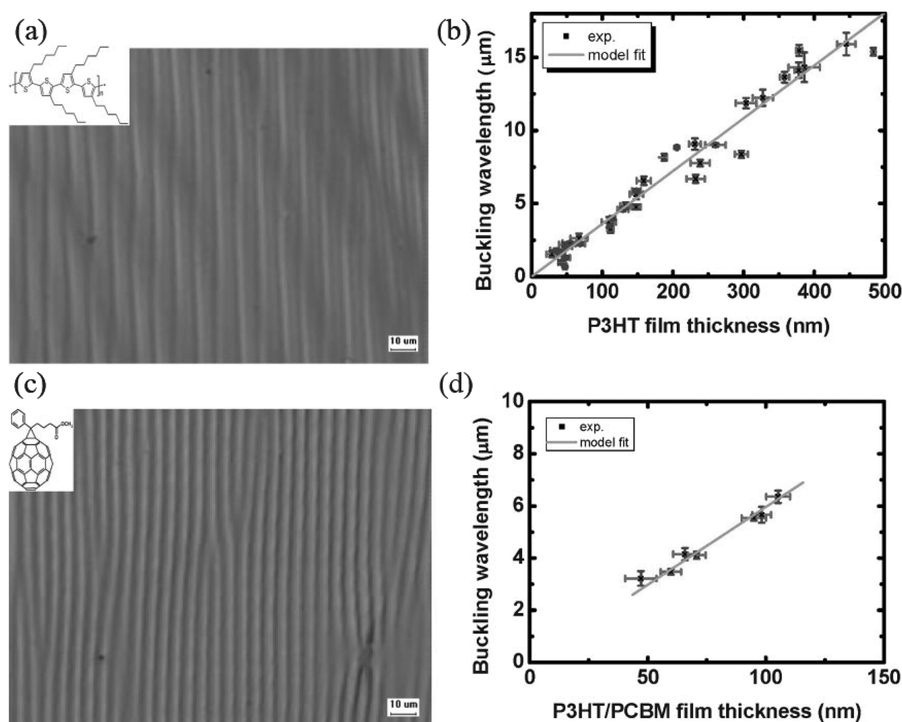

Fig. 13. Mechanical modulus of P3HT and P3HT/PCBM films.[45] Optical microscopy images for buckled P3HT and P3HT/PCBM films in (a) and (c), respectively. The insets show the chemical structure of P3HT and PCBM in the images. Measured wavelength data are plotted in (b) and (d), as a function of film thickness, where the green lines are fitted results.

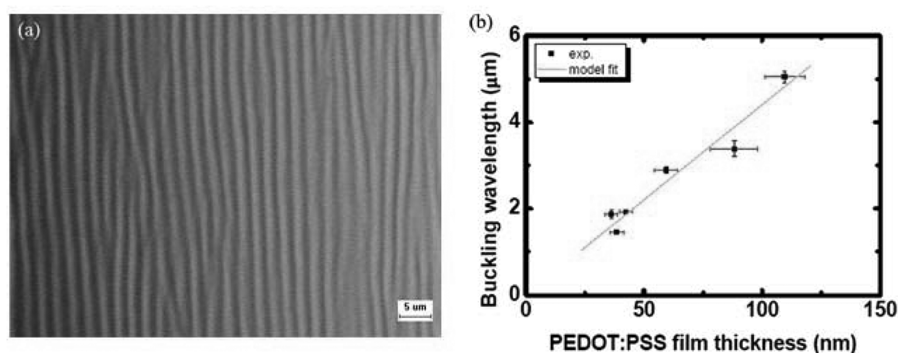

Fig. 14. (a) Optical microscopy image of buckled PEDOT:PSS film on elastomeric PDMS, and (b) experimental data of buckling wavelength as a function of film thickness.[45]

talline nature. Also, due to the relatively stiff nature of pentacene, delamination buckling is apparent (Fig. 15) when large compression (~10 %) is applied. Then other areas of pentacene film surface become flat, because the delamination buckles absorbs most of the applied compressive strain.

Another conducting polymer, PANI, shows a very small buckling wavelength of ~700 nm (Fig. 16). Thus the elastic modulus of PANI was found to be ~0.03 GPa. In the literature the value is 0.2 GPa to 2 GPa, depending on the fraction of residual solvent 1-methyl-2-pyrrolidone (NMP), which plays the role of plasticizer. Considering the higher content of residual NMP in the sample used in the experiment, the obtained ultralow modulus can be explained.

9. CONCLUDING REMARKS

Buckling-based measurements of mechanical moduli of various thin films and nano-scale materials are briefly reviewed in this work. The method proved to be quite effective in characterizing the mechanical properties of various materials, particularly materials in thin film form or at the nano-scale, which is difficult or impossible to do using other

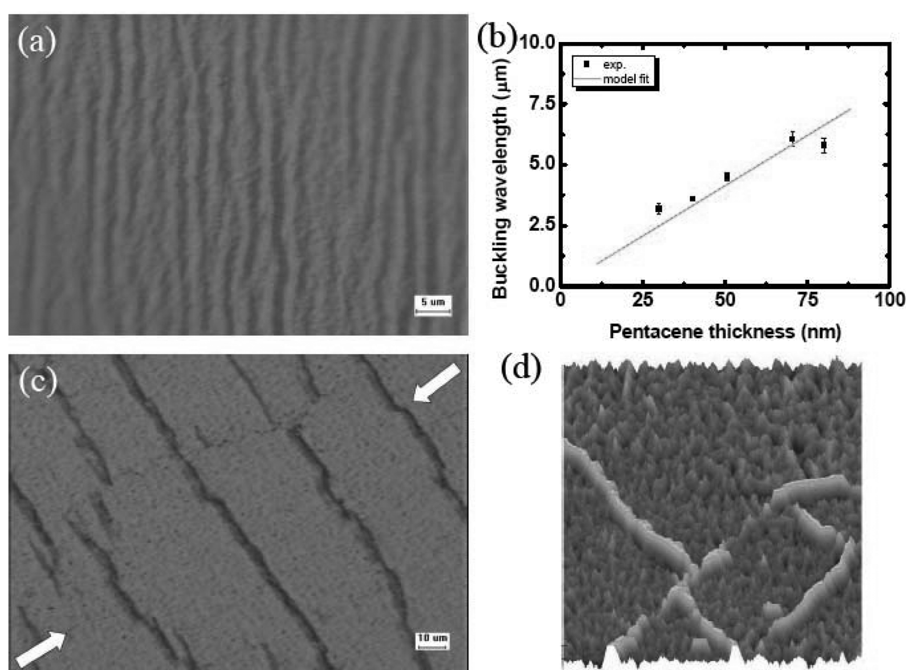

Fig. 15. (a) Optical micrograph image of buckled pentacene film on PDMS, (b) Young's modulus of pentacene film by fitting the experimental data with model equation, (c) the delaminated surface of pentacene film after applying and releasing high strain (~10 %), and (d) 3-dimensional atomic force microscopy image (50 μm × 50 μm, z-scale = 200 nm) of delaminated pentacene film on PDMS, such as shown in (c).[45]

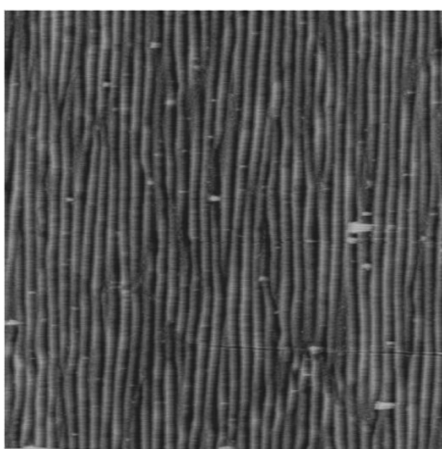

Fig. 16. AFM image of buckled surface of emeraldine base polyaniline (EB-PANI) layer on PDMS (30 μm × 30 μm, z-scale = 300 nm).[45]

methods. Also, the measured mechanical properties of those materials would be valuable for the successful implementation of flexible and/or stretchable electronics, where the mechanical properties of materials involved should be known for the device design, process optimization and other purposes.

ACKOWLEDGMENTS

The authors thank the financial support for this work from Korea Research Foundation (KRF) grant funded by the Korea government (MEST).

REFERENCES

1. S. Trolier-McKinstry, and P. Muralt, *J. Electroceramics.* **12**, 7 (2004).
2. S. H. Yi, H. C. Cho, and S. O. Han, *Electron. Mater. Lett.* **5,** 55 (2009).
3. Y. Zhao, J. Wang, and G. Mao, *Optics Lett*. **30**, 1885 (2005).
4. P. Muralt, *J. Micromech. Microeng*. **10**, 136 (2000).
5. P. Mitra, A. P. Chatterjee, and H. S. Maiti, *Mater. Lett*. **35**, 33 (1998).
6. H.-S. Hong and C.-O. Park, *Electron. Mater. Lett.* **1**, 11 (2005).
7. E. M. Kim, S. H. Min, and J. S. Jung, *Electron. Mater. Lett.* **3**, 217 (2007).
8. C. D. Dimitrakopoulos and P. R. L. Malenfant, *Adv. Mater.* **14**, 99 (2002).
9. D. A. Hardwick, *Thin Solid Films* **154**, 109 (1987).
10. M. Alcoutlabi and G. B. McKenna, *J. Phys.:Condens. Matter* **17**, R461 (2005).
11. S. Mahajan, *Electron. Mater. Lett.* **2**, 59 (2006).
12. S. W. Chung, S. Makhar, H. Ackler, and S. B. Park, *Electron. Mater. Lett.* **2**, 175 (2006).
13. J.-H. Zhao, M. Kiene, C. Hu, and P. S. Ho, *Appl. Phys. Lett*. **77**, 2843 (2000).
14. H. Y. Lee, S. J. Suh, S. R. Kim, S. Y. Park, and Y. C. Joo,

Electron. Mater. Lett. **2**, 175 (2009).
15. L. Sun and J. R. Dutcher, L. Giovannini and F. Nizzoli, J. R. Stevens, and J. L. Ord, *J. Appl. Phys*. **75**, 7482 (1994).
16. R. Hartschuh, Y. Ding, J. H. Roh, A. Kisliuk, A. P. Sokolov, C. L. Soles, R. L. Jones, T. J. Hu, W. L. Wu, and A. P. Mahorowala, *J. Polym. Sci., Part B: Polym. Phys*. **42**, 1106 (2004)
17. J. A. Forrest, K. Dalnoki-Veress, and J. R. Dutcher, *Phys. Rev. E* **58**, 6109 (1998).
18. S. A. Syed Asif, K. J. Wahl, and R. J. Colton, *Rev. Sci. Instrum*. **70**, 2408 (1999).
19. R. Saha and W. D. Nix, *Acta Mater.* **50**, 23 (2002).
20. A. A. Volinsky, J. B. Vella, and W. W. Gerberich, *Thin Solid Films* **429**, 201 (2003).
21. J. Y. Kim, Y. H. Lee, J. I. Jang, and D. I. Kwon, *Electron. Mater. Lett.* **2**, 139 (2006).
22. C. Escoffier, J. de Rigal, A. Rochefort, R. Vasselet, J.-L. Leveque, and P. G. Agache, *J. Inves. Derma.* **93**, 353 (1989).
23. D. Gazit, *Phy. Rev. B* **79**, 113411 (2009).
24. S. Srivastava and J. K. Basu, *Phy. Rev. E* **79**, 041603 (2009).
25. E. Cerda, and L. Mahadevan, *Phy. Rev. Lett.* **90**, 074302 (2003).
26. J. Genzer, and J. Groenewold, *Soft Matt.* **2**, 310 (2006).
27. A. L. Volynskii, S. Bazhenov, O. V. Lebedeva, and N. F. Bakeev, *J. Mater. Sci.* **35**, 547 (2000).
28. J. Groenewold, *Physica A*, **298**, 32 (2001).
29. N. Bowden, S. Brittain, A. G. Evans, J. W. Hutchinson, and G. M. Whitesides, *Nature* **393**, 146 (1998).
30. D.-Y. Khang, J. A. Rogers and H. H. Lee, *Adv. Funct. Mater.* **19**, 1526 (2009).
31. C. M. Stafford, C. Harrison, K. L. Beers, A. Karim, E. J. Amis, M. R. Vanlandingham, H. C. Kim, W. Volksen, R. D. Miller, and E. E. Simonyi, *Nat. Mater.* **3**, 545 (2004).
32. C. M. Stafford, B. D. Vogt, C. Harrison, D. Julthongpiput, and R. Huang, *Macromolecules* **39**, 5095 (2006).
33. A. J. Nolte, M. F. Rubner, and R and E. Cohen, *Macromolecules* **38**, 5367 (2005).
34. S. S. Shiratori and M. F. Rubnet, *Macromolecules* **33**, 4213 (2000).
35. A. J. Nolte, R. E. Cohen, and M. F. Rubner, *Macromolecules* **39**, 4841 (2006).
36. H. Hillborg, N. Tomczak, A. Olah, H. Schonherr, and G. J. Vancso, *Langmuir* **20**, 785 (2004).
37. A. Olah, H. Hillborg, G. J. Vancso, *Appl. Surf. Sci*. **239**, 410 (2005).
38. H. Huang, J. Y. Chung, A. J. Nolte, and C. M. Stafford, *Chem. Mater.* **19**, 6555 (2007).
39. E. A. Wilder, S. Guo, S. L. Gibson, M. J. Fasolka and C. M. Stafford, *Macromolecules* **39**, 4138 (2006).
40. J. Y. Chung, T. Q. Chastek, M. J. Fasolka, H. W. Ro, and C. M. Stafford, *ACS Nano* **3**, 844 (2009).
41. D.-Y. Khang, J. Xiao, C. Kocabas, S. MacLaren, T. Banks, H. Jiang, Y. Y. Huang, and J. A. Rogers, *Nano Lett*. **8**, 124 (2008).
42. K. S. Novoselov, A. K. Geim, S. V. Morozov, D. Jiang, Y. Zhang, S. V. Dubonos, I. V. Grigorieva, and A. A. Firsov, *Science* **306**, 666 (2004).
43. C. Berger, Z. Song, X. Li, X. Wu, N. Brown, C. Naud, D. Mayou, T. Li, J. Hass, A. N. Marchenkov, E. H. Conrad, P. N. First, W. A. de Heer, *Science* **312**, 1191 (2006).
44. M. J. Schultz, X. Zhang, S. Unarunotai, D.-Y. Khang, Q. Cao, C. Wang, C. Lei, S. MacLaren, J. A. N. T. Soares, I. Petrov, J. S. Moore, and J. A. Rogers, *PNAS* **105**, 7353 (2008).
45. D. H. Tahk, H. H. Lee, and D.-Y. Khang, *Macromolecules* **42**, 7079 (2009).